

Spectroscopy of the anharmonic cantilever oscillations in tapping-mode atomic-force microscopy

Martin Stark^{a)}

Max-Planck-Institut für Biochemie, Abt. Molekulare Strukturbiologie, D-82152 Martinsried, Germany

Robert W. Stark^{b)} and Wolfgang M. Heckl

Universität München, Institut für Kristallographie und Angewandte Mineralogie, Theresienstr. 41, 80333 München, Germany

Reinhard Guckenberger

Max-Planck-Institut für Biochemie, Abt. Molekulare Strukturbiologie, D-82152 Martinsried, Germany

(Received 17 July 2000; accepted for publication 22 September 2000)

By spectroscopic analysis of the cantilever oscillation in tapping-mode atomic-force microscopy (TM-AFM), we demonstrate that the transition from an oscillatory state dominated by a net attractive force to the state dominated by repulsive interaction is accompanied by the enhanced generation of higher harmonics. The higher harmonics are a consequence of the nonlinear interaction and are amplified to significant amplitudes by the eigenmodes of the cantilever. The results show that in a quantitative description of TM-AFM higher eigenmode excitation must be considered to account for internal energy dissipation. © 2000 American Institute of Physics. [S0003-6951(00)01946-X]

For spatially resolved surface characterization on the nanometer-scale, several quasistatic (for reviews see, e.g., Refs. 1 and 2) and dynamic³⁻⁶ operation modes were developed for atomic-force microscopy (AFM). In tapping-mode AFM (TM-AFM),⁷ the cantilever is excited to oscillate close to its resonance. Contrast mechanisms and dynamics of TM-AFM have been investigated by several groups. It was shown, that the phase lag between excitation and response of the cantilever is related to the energy dissipated in the tip-sample contact.^{8,9} A profound description of the role of conservative and dissipative interaction forces in the tip-sample contact is given in Refs. 10 and 11.

Several authors report on a discontinuity in the oscillation amplitude in TM-AFM during the approach to the sample, which is related to the transition from an oscillatory state dominated by attractive interaction to a state dominated by repulsive forces.¹²⁻¹⁴ From a numerical one-degree-of-freedom approximation it was found that both solutions coexist.^{15,16} Recently, the forces at this transition were measured directly.¹⁷

In TM-AFM nonlinearities occur, because the sample surface confines the cantilever motion on one side at the tip sample contact. Numerical simulations predict period doubling^{18,19} for some cases. Higher harmonics of the working frequency are introduced by the nonlinearities and are amplified to significant amplitudes by the internal resonances of the higher eigenmodes of the cantilever beam which lead to the suggestion of a Fourier-transformed AFM.^{20,21} For several comparable macroscopic impact oscillators, like single-degree-of-freedom oscillators (e.g., Refs. 22-24) and macroscopic beams (e.g., Ref. 25) the nonlinear nature of the dynamics was investigated in detail. It was shown that the

evolution of the dynamical system in time depends on the discrete stiffness of the sample as well as on damping nonlinearities.^{26,27}

Comparing macroscopic impact oscillators with TM-AFM, it is important to note that the relative time scale of the interactions differ. In TM-AFM the interaction time is a considerable fraction of the cycle time,^{28,21} whereas in macroscopic systems the impact can be considered to be infinitely short (e.g., Ref. 25).

In the following we demonstrate that at the transition from the oscillatory state dominated by net attractive forces to the state dominated by repulsive forces enhanced higher harmonics generation occurs, coupled to higher eigenmode excitation. Thus, an adequate description of TM-AFM must account for the cantilever beam. An exact knowledge of the oscillatory motion of the nonlinear system is important for the application of TM-AFM in quantitative surface characterization, high-resolution imaging as well as dynamical nano-structuring^{29,30} where it is an essential to control the tip-sample interaction forces.

For the experimental investigation, a commercial AFM³¹ was equipped with a standard silicon cantilever.³² The cantilever was driven at its resonant frequency $f_0 = 44.86$ kHz. The photodiode signal monitoring the motion of the tip interacting with a silicon (100) surface under ambient conditions was recorded together with the driving voltage using an analog-to-digital converter³³ at a sampling rate of 5 M samples/s. The signals were analyzed off-line.

First, enhanced higher harmonics generation at the transition from attractive to repulsive dominated state shall be demonstrated. Figure 1 shows the amplitude dependence of the fundamental oscillation during the approach. In the amplitude signal (A), as well as in the phase-signal (Φ) the transition between the attractive (a) and repulsive (r) state can clearly be identified. The respective spectra in Fig. 2

^{a)}Author to whom correspondence should be addressed; electronic mail: stark@biochem.mpg.de

^{b)}Electronic mail: robert@nanomanipulation.de

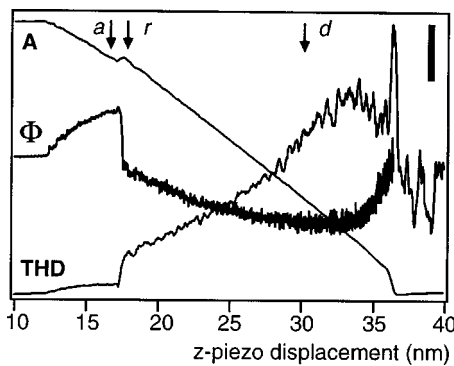


FIG. 1. Approach curves on a Si(100) sample: amplitude A of the fundamental, phase Φ , and total harmonic distortion THD. The arrows indicate the tip-sample separation where the spectra and phase space trajectories were taken: a attractive, r repulsive, and d deep repulsive. Scaling bars: amplitude 100 mV, phase 36° , and THD 4%.

were obtained at the points marked by arrows (a and r , respectively) in Fig. 1. In the attractive regime, higher harmonics contributed only with small amplitudes to the signal [Fig. 2(a)]. In the repulsive state, significant excitation of higher harmonics occurs due to the repulsive interaction [Fig. 2(b)]. The harmonics are grouped around the resonant frequencies of the eigenmodes No. 3 (239.7 kHz) and No. 5 (563.2 kHz, nomenclature according to Ref. 34) of the cantilever.²¹

The enhanced higher harmonics generation in the repulsive state can qualitatively be understood, describing the impact in Fourier space. The narrow in time (but compared to the attractive forces strong) repulsive force pulse extends over a broad frequency band in Fourier space. These frequencies couple to higher eigenmodes. The periodicity of the impact then leads to the observed discrete spectra. A more rigid description can be found in Ref. 20.

The total harmonic distortion (THD) (as defined by the American National Standards Institute) provides a measure for the fraction of power transferred from the fundamental into higher harmonics. It can adopt values between 0% and 100%. For the photodiode signal S , which measures the deflection angle of the cantilever but not the tip-displacement itself, the THD is given by

$$\text{THD} = \sqrt{\frac{\sum_{n=2}^{\infty} U_n^2}{\sum_{n=1}^{\infty} U_n^2}} \times 100\%, \quad (1)$$

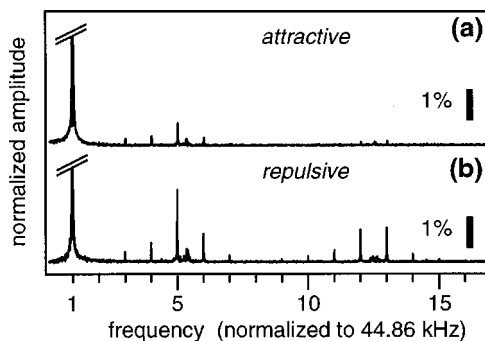


FIG. 2. Spectra of the photodiode signal. (a) In the attractive state, small contributions of higher harmonics are visible. (b) In the repulsive state a significant distortion from harmonic behavior becomes apparent. (Amplitudes normalized to the fundamental.)

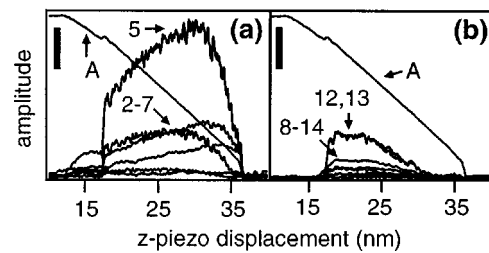


FIG. 3. Approach curves of the higher harmonics in the photodiode signal together with the amplitude A of the fundamental. (a) Harmonics 2–7, that can be attributed to the internal resonance of eigenmode No. 3. The fifth harmonic prevails. (b) Harmonics 8–14, enhanced by mode No. 5 with the 12th and 13th harmonic dominating. Scaling bar: 5 mV (100 mV for the amplitude of the fundamental).

where U_n is the root-mean-square amplitude of the voltage of the n th harmonic. In Fig. 1 the THD is shown as a function of the z -piezo displacement. The transition from the attractive to the repulsive state dominated by short-range and strongly repulsive forces coincides with a discontinuity in the signals A , Φ , and in the THD. The THD of the photodiode signal increases further during the approach, indicating that the photodiode signal becomes more distorted. Here, a maximum of $\text{THD} = 15\%$ was measured.

To obtain the fraction of oscillation energy transferred per cycle into the higher harmonics [$\text{THD}(E)$], the diode signal must be corrected for the geometrical enhancement of the contribution of higher eigenmodes, and the effective spring constants of the respective eigenmodes have to be used.³⁵ The $\text{THD}(E)$ exhibits a maximum of $\text{THD}(E) = 5\%$. This clearly shows that the energy transfer into higher order oscillations can constitute a channel for significant internal energy dissipation as was inferred earlier.³⁴

The absolute deflection-signal amplitudes of the different harmonics as a function of the z -piezo displacement are shown in Fig. 3. Harmonics number 5, as well as 12 and 13, which are close to eigenmode frequencies, are most prominent which illustrates the amplification due to internal resonances of the system. There is a discontinuity prominent in the amplitude of the higher harmonics, that coincides with the transition from the attractive to the repulsive regime.

Visualizing the cantilever motion in phase space (Fig. 4, the sample surface is to the left), the increasing complexity of the motion can be seen. The trajectory is projected on a plane with the photodiode signal S and its time derivative \dot{S} as coordinates³⁶ associated to deflection angle and angular momentum at the free end of the cantilever, respectively. For clarity, the points representing the state of the motion at each discrete sampling time are not connected. For the free oscil-

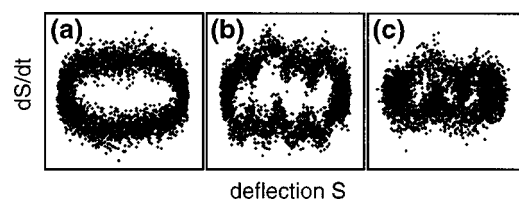


FIG. 4. Projections of the experimentally determined trajectories in phase space in the S - \dot{S} plane. (a) attractive regime; (b) repulsive regime; and (c) close to maximum THD (deep repulsive). Full scales: S : -0.5 – 0.5 V [(a) and (b)], -0.25 – 0.25 V (c); and \dot{S} : -250 – 250 mV/s for all.

lation (not shown), the trajectory in the $S-\dot{S}$ plane is elliptic, as expected for a harmonic oscillator. In the attractive state [Fig. 4(a)], the trajectory deviates only slightly from the free oscillation. Regarding the repulsive dominated state [Fig. 4(b)], obvious deviations from the basic ellipse caused by nonlinear perturbation and associated to enhanced higher-harmonic generation become prominent. Even though the system is strongly nonlinear close to maximum THD (marked with d in Fig. 1), it still follows a one-periodic (nonchaotic) orbit in phase space [Fig. 4(c); note the reduced range of S].

In conclusion we demonstrated enhanced higher harmonics generation at the transition from attractive to repulsive dominated oscillatory state, accompanied by a significant fraction of energy transferred to higher eigenmodes. The higher harmonics can be used as on-line indicative qualifying the interaction forces and may even be used as input in the feedback loop.

Furthermore, the experimental results show that higher eigenmode excitation is an important feature in TM-AFM. Thus, a multiple-degree-of-freedom description is essential for a quantitative understanding of the dynamics and to apply TM-AFM as a surface characterization tool.

The authors thank Dr. Ricardo García (Instituto de microelectrónica, Madrid, Spain), Rainer Hillenbrand (MPI für Biochemie, Germany), Dr. Ferdinand Jamitzky, and Tanja Drobek (LMU, Munich, Germany) for stimulating discussions. Financial support by the Deutsche Forschungsgemeinschaft (SFB266; MS) and by Grant No. BMBF 13N7509/1 (RWS) are gratefully acknowledged.

¹L. A. Bottomley, J. E. Coury, and P. N. First, *Anal. Chem.* **68**, R185 (1996).

²G. Friedbacher and H. Fuchs, *Pure Appl. Chem.* **71**, 1337 (1999).

³M. Radmacher, R. W. Tilmann, and H. E. Gaub, *Biophys. J.* **64**, 735 (1993).

⁴U. Rabe and W. Arnold, *Appl. Phys. Lett.* **64**, 1493 (1994).

⁵O. V. Kolosov, M. R. Castell, C. D. Marsh, and A. Brix, *Phys. Rev. Lett.* **81**, 1046 (1998).

⁶T. Drobek, R. W. Stark, M. Gräber, and W. Heckl, *New J. Phys.* **1**, 15.1 (1999).

⁷Q. Zhong, D. Inniss, K. Kjoller, and V. B. Elings, *Surf. Sci.* **290**, L688 (1993).

⁸S. N. Magonov, V. Elings, and M. H. Whangbo, *Surf. Sci.* **375**, L385 (1997).

⁹J. P. Cleveland, B. Anczykowski, A. E. Schmid, and V. B. Elings, *Appl. Phys. Lett.* **72**, 2613 (1998).

¹⁰U. Dürig, *Appl. Phys. Lett.* **76**, 1203 (2000).

¹¹U. Dürig, *New J. Phys.* **2**, 5.1 (2000).

¹²P. Gleyzes, P. K. Kuo, and A. C. Boccara, *Appl. Phys. Lett.* **58**, 2989 (1991).

¹³B. Anczykowski, D. Krüger, K. L. Babcock, and H. Fuchs, *Ultramicroscopy* **66**, 251 (1996).

¹⁴A. Kühle, A. Sorensen, and J. Bohr, *J. Appl. Phys.* **81**, 6562 (1997).

¹⁵R. García and A. San Paulo, *Phys. Rev. B* **60**, 4961 (1999).

¹⁶R. García and A. San Paulo, *Phys. Rev. B* **61**, R13381 (2000).

¹⁷S. C. J. Fain, K. A. Barry, M. G. Bush, B. Pittenger, and R. N. Louie, *Appl. Phys. Lett.* **76**, 930 (2000).

¹⁸J. P. Hunt and D. Sarid, *Appl. Phys. Lett.* **72**, 2969 (1998).

¹⁹N. Sasaki, M. Tsukada, R. Tamura, K. Abe, and N. Sato, *Appl. Phys. A: Mater. Sci. Process.* **66**, S287 (1998).

²⁰R. W. Stark and W. M. Heckl, *Surf. Sci.* **457**, 219 (2000).

²¹R. Hillenbrand, M. Stark, and R. Guckenberger, *Appl. Phys. Lett.* **76**, 3478 (2000).

²²S. W. Shaw and P. J. Holmes, *J. Sound Vib.* **90**, 129 (1983).

²³A. B. Nordmark, *J. Sound Vib.* **145**, 275 (1991).

²⁴C. N. Babpat, *J. Sound Vib.* **209**, 43 (1998).

²⁵D. J. Wagg, G. Karpodinis, and S. R. Bishop, *J. Sound Vib.* **228**, 243 (1999).

²⁶C. J. Begeley and L. N. Virgin, *J. Sound Vib.* **211**, 801 (1998).

²⁷L. N. Virgin and C. J. Begeley, *Physica D* **130**, 43 (1999).

²⁸J. Tamayo and R. García, *Langmuir* **12**, 4430 (1996).

²⁹B. Klehn and U. Kunze, *Superlattices Microstruct.* **23**, 441 (1998).

³⁰R. W. Stark, S. Thalhammer, J. Wienberg, and W. M. Heckl, *Appl. Phys. A: Mater. Sci. Process.* **66**, S579 (1998).

³¹Multimode, Nanoscope III, Veeco (Digital Instruments), Santa Barbara, CA.

³²NSC 21, Silicon, manufacturer's data: $k=1.4\text{ N/m}$ (NT-MDT, Moscow, Russia).

³³DAQCard-AI-16E-4, National Instruments Corp., Austin, TX.

³⁴R. W. Stark, T. Drobek, and W. M. Heckl, *Appl. Phys. Lett.* **74**, 3296 (1999).

³⁵R. W. Stark, T. Drobek, and W. M. Heckl, *Ultramicroscopy* (to be published).

³⁶This set of coordinates was found to be most instructive, other choices for coordinates are possible yielding the same result.